Article:

Zhuo, L. orcid.org/0000-0002-5719-5342, Dai, Q., Han, D. et al. (3 more authors) (2019) Evaluation of remotely sensed soil moisture for landslide hazard assessment. IEEE Journal of Selected Topics in Applied Earth Observations and Remote Sensing, 12 (1). pp. 162-173. ISSN 1939-1404

https://doi.org/10.1109/jstars.2018.2883361

Evaluation of Remotely Sensed Soil Moisture for Landslide Hazard Assessment

Lu Zhuo, Qiang Dai, Dawei Han, Ningsheng Chen, Binru Zhao, Matteo Berti

Abstract—Soil moisture is important in the triggering of many types of landslides. However, in-situ soil moisture data are rarely available in hazardous zones. The advanced remote sensing technology could provide useful soil moisture information. In this study, an assessment has been carried out between the latest version of the European Space Agency Climate Change Initiative soil moisture product and the landslide events in a northern Italian region in the 14-year period 2002-2015. A clear correlation has been found between the satellite soil moisture and the landslide events, as over four-fifths of events had soil wetness conditions above the 50% regional soil moisture line. Attempts have also been made to explore the soil moisture thresholds for landslide occurrences under different environmental conditions (land cover, soil type, and slope). The results showed slope distribution could provide a rather distinct separation of the soil moisture thresholds, with thresholds becoming smaller for steeper areas, indicating dryer soil condition could trigger landslides at hilly areas than in plain areas. The thresholds validation procedure is then carried out. 45 rainfall events between 2014-2015 are used as test cases. Contingency tables, statistical indicators, and Receiver Operating Characteristic analysis for thresholds under different exceedance probabilities (1% - 50 %) are explored. The results have shown that the thresholds using 30% exceedance probability provide the best performance with the hitting rate at 0.92 and the false alarm at 0.50. We expect this study can provide useful information for adopting remotely sensed soil moisture in the landslide early warnings.

Index Terms—Emilia Romagna, European Space Agency (ESA) Climate Change Initiative (CCI) v04.2, landslide, natural hazards, satellite remote sensing, soil moisture.

I. INTRODUCTION

LANDSLIDE is one of the most common and dangerous natural hazards worldwide, causing severe direct impacts on human lives, public and private properties and lifelines [1]. Moreover it can lead to indirect damages to the whole society, ranging from the reduction of productivity force, a decline of industrial revenue to mental trauma and the break of an economic system [2-4]. Early warnings and predictions are therefore essential for mitigating such impacts. The most common way of real-time landslide forecasting relies on rainfall thresholds, which has been adopted worldwide due to its simplicity [5]. However, in many cases, early warnings based solely on rainfall is not adequate, because soil moisture conditions play a crucial role in the initiation of landslides [6-13].

Although the importance of soil moisture condition has been widely recognized in landslides forecasting, the direct usage of soil moisture data in the area is still limited. In most cases, only the antecedent precipitation indices (i.e., precipitation accumulated during a given period before landslide triggered; [14-16]) are adopted to approximate soil moisture. However, such an approach is not recommended by many studies due to the weak relationships found between the antecedent precipitation and the real soil moisture variations [17-19]. This is due to not all precipitation enters the soil layer when reaching the earth surface, instead, parts of them become direct runoff [20, 21]. In addition, evapotranspiration plays an important role in the soil moisture temporal evolution, which also leads to the weak relationships as aforementioned. Therefore, it is important to use the actual soil moisture information for landslide studies.

Generally, soil moisture can be estimated through in-situ measurements, models, and remote sensing. In-situ measurements can provide the highest accuracy among all the three methods, but it only gives point-based measurements. Since soil moisture has a high variability in both space and time especially in steep mountainous areas, a dense soil moisture network is normally required at those high-risk areas for monitoring purposes. Some studies have been carried out to explore the usefulness of in-situ soil moisture for landslide applications [9, 18, 22, 23]. Unfortunately, in many remote areas, soil moisture stations are not available or only are sparsely distributed in those non-hazardous areas, due to high installation and maintenance cost (e.g., in our study area, although there is a total of 19 in-situ soil moisture sensors

This study is supported by Resilient Economy and Society by Integrated SysTems modelling (RESIST), Newton Fund via Natural Environment Research Council (NERC) and Economic and Social Research Council (ESRC) (NE/N012143/1), and the National Natural Science Foundation of China (No: 4151101234). (Corresponding author: Qiang Dai.)

Lu Zhuo and Dawei Han are with WEMRC, Department of Civil Engineering, University of Bristol, Bristol, UK (email: lu.zhuo@bristol.ac.uk, d.han@bristol.ac.uk).

Qiang Dai is with Key Laboratory of VGE of Ministry of Education, Nanjing Normal University, Nanjing, China; and is currently a visiting post-doc in WEMRC, Department of Civil Engineering, University of Bristol, Bristol, UK (email: civengwwater@gmail.com).

Ningsheng Chen is with The Institute of Mountain Hazards and Environment (IMHE), China (chennsh@imde.ac.cn).

Binru Zhao is with College of Water Conservancy and Hydropower Engineering, Hohai University, Nanjing, China, and is currently a visiting PhD student in WEMRC, Department of Civil Engineering, University of Bristol, Bristol, UK (binru.zhao@bristol.ac.uk).

Matteo Berti is with Department of Biological, Geological, and Environmental Sciences, University of Bologna, Piazza di Porta S.Donato 1, Bologna, Italy (matteo.berti@unibo.it)

installed, nearly all of them are installed in the plain areas where landslides never occurred). Another technique to obtain continuous soil moisture variations relies on land surface /hydrological modelling [7, 24-27]. However, model-based methods tend to suffer from time drifts problem (e.g., error accumulation over times), require a large number of accurate data inputs and are normally computationally intensive particularly for large monitoring areas. Alternatively, remote sensing is an advanced technology in soil moisture monitoring on a global scale [28-30]. There have been enormous investments by various organisations such as ESA (European Space Agency), NASA (National Aeronautics and Space Administration) and EUMETSAT (European Organisation for the Exploitation of Meteorological Satellites), in a wide range of soil moisture observational programs (e.g., ENVISAT (Environmental Satellite), ASCAT (Advanced Scatterometer), AMSR-E (Advanced Microwave Scanning Radiometer for EOS), SMOS (Soil Moisture and Ocean Salinity), and SMAP (Soil Moisture Active Passive)). However, despite their free availabilities, studies attempting to use them for landslide-related applications are nearly absent [25]. To our knowledge so far only five pioneering studies have been carried out by Brocca et al. (2016; 2012) [25, 31] with ASCAT, and Ray and Jacobs, (2007), Ray et al., (2011; 2010) [32-34] with AMSR-E, which all have illustrated the effectiveness of utilising satellite soil moisture for landslide predictions and monitoring, despite coarse resolution and the shallow soil depth sensed by satellite sensors . Such a significant gap between the satellite soil moisture data abundancy and the landslide studies scarcity demonstrates the necessity of further research in this area. Particularly, since more satellite soil moisture data are becoming available, further studies using different data sources should be carried out. On the other hand, soil moisture thresholds can be useful information for landslide hazards early warnings (e.g., to work together with rainfall thresholds), however such a research has rarely been carried out [25, 35].

Therefore, the aim of this paper is to further explore the usefulness of remotely sensed soil moisture products for landslide applications with the latest satellite soil moisture data. In addition, it is attempted to investigate the soil moisture triggering conditions for landslide occurrences based on different environmental features (i.e., land cover, soil type, slope), as using only one threshold for a large study area is not appropriate [36], after which, thresholds are validated statistically. Here the state-of-the-art ESA Climate Change Initiative (CCI) soil moisture product (CCI-SM hereafter) is chosen because the program is the first of its kind in merging multiple active and passive microwave sensors to produce a long-term (>30 years), harmonized satellite soil moisture datasets [37]. CCI-SM has been demonstrated with good agreements with the in-situ observations globally [38-40]. The large physiographic variability, together with the maturity of landslide data records, make Italy an ideal place for this study. Here an Italian region called Emilia Romagna is chosen for this purpose. The study period is from 2002 to 2015, where both the landslide records and the CCI-SM datasets are the most complete. Details regarding the study area, and different data used are provided in Section II. Methodologies for thresholds validation are described in Section III. The satellite soil moisture evaluation result is covered in Section IV. Section V shows the landslide relationships with the satellite soil moisture. The attempts of exploring soil moisture thresholds as well as their validations are presented in Section VI. Section VII includes further discussions about the results, potential future works, and conclusions.

II. Study Area and Datasets

A. Study Area

The Emilia Romagna Region is located in the north of Italy and is one of the country's most populated areas (Figure 1). The region's topography changes from hilly and mountainous sectors in S-SW to wide plains towards NE, and its elevation can vary from 50 m up to 2125 m over a distance approximately 50 km running north to south [41, 42]. The mountainous part (about 13,200 km^2) belongs to the northern Apenines chain, which is a complex fold and thrust arcuate orogenic belt that was formed due to the closure of the Ligurian Ocean and the subsequent collision of the European and continental margins which started in the Oligocene.

The region has a mild Mediterranean climate with distinct warm and dry season from May to October, and a cool and wet season from November to April. The mean annual rainfall averaged over the whole area is about 1000 mm, but it can reach around 2000 mm in the highest mountains. The Emilia Romagna Region is extremely prone to landslides, with one-fifth of the hilly and mountainous territory covered by active or dormant landslide deposits. The majority of them were caused by earth-flows after the Last Glacial Maximum and the expansion during the wet seasons of the Holocene which created superimposition of new earth-flows. Intense and prolonged rainfall events are the main triggering factors for reactivation of those pre-existing deposits, followed by snow melted by warm rain. Although the landslides in the area do not normally cause casualties, they lead to a considerable number of damages to the properties and local infrastructures. Each year the cost for the purpose of property rebuilt and area regeneration is around €33 million.

B. The CCI-SM Products

The first version of the CCI-SM was released in 2012, which was the first multi-decadal, global satellite-observed soil moisture product. It is produced by merging information from both active and passive microwave space-borne instruments, into three harmonised products: a merged ACTIVE (1991-2016), a merged PASSIVE (1978-2016), and a COMBINED (1978-2016) active + passive microwave product. Compare with its first release, the latest version which is adopted in this study (v04.2, released in early 2018) includes a large number of advancements, for instance incorporates various new satellites, extends temporal coverage to 1978-2016, merges all active and passive Level-2 products directly to generate the COMBINED product (previously, this was created from the ACTIVE and PASSIVE products) [43], and uses a new blending approach to compute a weighted average of measurements from all sensors that are available at a certain point in time. Comparatively, microwave bands have more advantages in soil moisture estimation than other spectral bands, mainly because they have longer wavelengths, so they can penetrate deeper into the soil and have more ability to pass through cloud and some vegetation cover [21]. As a result, CCI-SM can provide soil moisture information in the upper few centimetres of soil. CCI-SM is in the format of volumetric water content (m^3/m^3), with a daily temporal resolution, and 0.25-degree spatial resolution globally.

The active data used in the newest version of the CCI-SM are generated by the Vienna University of Technology (TU Wien) based on observations from the C-band scatterometers on board of the European remote sensing satellite-1 (ERS-1), ERS-2 and Meteorological operational satellite – A (MetOp-A) and MetOp-B. The passive data set are produced by the VU University Amsterdam in collaboration with NASA based on passive microwave observations from Nimbus 7 Scanning Multi-channel Microwave Radiometer (SMMR), Defense Meteorological Satellite Program (DMSP) Special Sensor Microwave Imager (SSM/I), Tropical Rainfall Measuring Mission's (TRMM) Microwave Imager (TMI), Aqua AMSR-E, Coriolis WindSat, Global Change Observation Mission-Water "Shizuku" (GCOM-W1) AMSR2, and SMOS. The CCI-SM is continuously being upgraded, although SMAP is not currently considered, it is expected to be included in its future releases. In this study, the CCI-SM COMBINED product is used.

C. Landslide Database Discrimination

The adopted historical landslides catalog is from the Emilia Romagna Geological Survey, which holds a large collection of landslides data sourced from parochial archives, technical documentation, reports to local authorities, national, regional and local newspapers [41]. The catalog only contains records of landslides that caused damages, therefore small-sized ones occurred in remote areas were likely to be undetected. Although the catalog does not contain all the occurred landslides information it is an accurate inventory of those that caused certain damages. The information in the catalog includes location, date of occurrence, the uncertainty of date, landslide characteristics (dimensions, type, and material), triggering factors, damages, casualties, and references. Unfortunately, the complete information is not available for all the landslides and in many cases, they are missing. Based on the available information, two rules are set to decide if a landslide data could be used for the analysis purpose: 1) rainfall-induced only; 2) the time of occurrence should be in daily accuracy. Moreover the catalog period for the selection process is between 2002 and 2015 only, which is during the period when CCI-SM is the most complete. Given these restrictions, about four-fifths of data cannot fulfil them and were hence deleted. As a result, a total of 239 events are retained. The individually retained landslides are mapped as single pinpoints in Figure 2, with Digital elevation model (DEM) information also shown in the background. The spatial distribution of landslides is very heterogeneous, and it is controlled by the distribution of the weak rock units as well as by the location of the critical rainfall events during the considered period.

D. Other Datasets

1) In-situ data

Among the 19 installed in-situ soil moisture sensors within the study area, only one sensor installed at San Pietro Capofiume (latitude 44° 39' 13.59", longitude 11° 37' 21.6") provides long-term surface soil moisture information (at 10 cm). The rest of the sensors are either absent from valid data (e.g., no data, or very big data gaps) or do not cover the study period at all. Therefore, only the San Pietro Capofiume station is used for the CCI-SM evaluation purpose. The San Pietro Capofiume site is typical of the agricultural area of the Po River valley. The soil moisture data measurements are carried out by the Regional Agency for Environmental Protection of Emilia Romagna Region at seven different depths in the soil between 10 cm and 180 cm. Time Domain Reflectometry (TDR) equipped with dataloggers is used for automatic data collection. The volumetric water content (m^3/m^3) has been recorded in a daily timestep between 2006 and 2017 [44]. Here only the data covered by the study period is collected (i.e., 2006-2015 for the evaluation of CCI-SM). The rain gauge network of the study area consists of over 200 tipping-bucket rain gauges. For the purpose of rainfall event selections, daily rainfall data covering the whole area are collected and analysed for years 2014 and 2015.

2) Environmental data

In addition to the soil moisture and landslide information, environmental features (i.e., land cover, soil type, and slope) are obtained from different sources. The reasons for choosing those features are because they have been found with important roles in landslide occurrences [45]. The ESA CCI land cover map (v2.0.7) is used here. The map describes the Earth's terrestrial surface in 37 original land cover classes at 300 m resolution. The classification is based on the United Nations Land Cover Classification System [46]. The reason for choosing the CCI land cover map is similar to the CCI-SM's because we aim to exploit the full range of available datasets from remote sensing technologies (i.e., from ESA and relevant European missions). The soil type map is from the SoilGrids-World Reference Base class (TAXNWRB), which categorises the world into 118 unique soil classes. SoilGrids is a system for automated soil mapping based on state-of-the-art spatial predictions methods. It provides a collection of updatable soil property and class maps of the world at 250 m spatial resolutions produced using automated soil mapping based on machine learning algorithms [47]. The slope information over the study region is calculated by using the Shuttle Radar Topography Mission (SRTM) 3 Arc-Second Global (~ 90m) DEM datasets. The reason for choosing SRTM DEM data is because it is of high quality and is the most used free DEM data worldwide. The coverage of this dataset is near global extending from 60° north to 56° south in latitude [48]. Although more detailed information of elevation, land use and soil type could be sourced for the study area, the global datasets are chosen here because they are freely available globally, which can make this study exportable worldwide.

III. METHODOLOGIES

In order to perform the calibration and validation of the soil moisture thresholds, landslides and CCI-SM datasets are divided into two periods: 2002-2013 for the construction of thresholds, and 2014-2015 for the validation purpose. The definition of soil moisture thresholds is based on finding the soil moisture triggering levels (thresholds) using different exceedance probabilities (percentiles), e.g., a 5% exceedance probability is based on calculating the 5% percentile value of the soil moisture observations in correspondence of the landslide events. The adoption of exceedance probability is a common way to determine rainfall-thresholds in the landslide early warning, which is therefore used in this study to explore its usage for soil moisture threshold determinations.

During the validation period, 45 rainfall events are selected as the test cases for the threshold's performances. To separate rainfall events from rainfall datasets, a one-day dry period (i.e., a period without rainfall) is used [49-51]. Since most of the landslides included in the datasets are shallow which respond quickly to rainfall, therefore a one-day approach is suitable here. The events generated through each rain gauge are then combined, and with visual analysis, the rainfall event periods for the whole study area are finally selected. The rainfall events data are shown in Section VI.

The validation methods used are based on Gariano et al. (2015) [52]. Here the soil moisture thresholds can be considered as a binary classifier of the soil moisture conditions that are likely or unlikely to lead to landslides. Based on such an assumption, the landslide occurrences can either be true (T) or false (F), and the threshold predictions can either be positive (P) or negative (N). As a result, there are four outcomes (Figure 3a), i.e., true positive (TP), true negative (TN), false positive (FP), and false negative (FN) [53]. A true positive is an outcome where the threshold correctly predicts the occurrences of landslides; similarly, a true negative is an outcome where the threshold correctly predicts the unoccurrences of landslides; a false positive (i.e., false alarm) is an outcome where the threshold is reached, but in reality landslides do not occur; and a false negative (i.e., missing alarm) is an outcome where threshold failed to predict the occurrences of landslides. Based on the four possible outcomes, three statistical indicators can be calculated.

The Hit Rate (HR), which is the proportion of the events that are correctly predicted. It can be calculated as:

$$HR = \frac{TP}{TP+FN} \tag{1}$$

ranges between 0 and 1, with the optimal value as 1.

The False Alarm Rate (FAR), which is the proportion of positive predictions when the event did not occur. It can be calculated as:

$$FAR = \frac{FP}{FP+TN} \tag{2}$$

ranges between 0 and 1, with the optimal value as 0.

TABLE I
PERCENTAGE OF LANDSLIDE EVENTS EXCEED THE GRID SOIL MOISTURE CONDITION AT DIFFERENT PERCENTILES.

Percentile (%)	Percentage of events exceeded (%)
95	24
90	41
80	52
70	72
60	79
50	83

The Hanssen and Kuipers skill score (HK) [54], which is the forecasting accuracy for the events with and without landslides. It can be calculated as:

$$HK = HR - FAR \tag{3}$$

ranges between -1 and 1, with the optimal value as 1.

The predicting performance of different exceedance probability levels is examined by using a Receiver Operating Characteristic (ROC) analysis [55, 56]. The analysis is based on the ROC plot with HR against FAR as seen in Figure 3b. Each point in the plot represents each exceedance probability level scenario. The optimal result (the red point) is achieved when the HR equals 1 and the FAR equals 0. The closer the point to the optimal performance point, the better the prediction ability is. Hence the Euclidean distances (d) between individual points and the optimal points are calculated to judge which scenario is the best.

For the validation study, each threshold determined for each of the slope class is used for summarising the numbers of T, F, P, and N events. Those numbers are then combined to determine the overall statistical indicators (i.e., HR, FAR, HK).

IV. RESULTS OF CCI-SM EVALUATION

To use the CCI-SM, the initial step is to evaluate its reliability. For this purpose, the CCI-SM is compared with the in-situ observations over the period of 2006 to 2015. Figure 4 illustrates the comparison result between the satellite and the in-situ soil moisture. It can be seen CCI-SM is able to monitor the overall seasonal and temporal changes of soil moisture. Only for some cases: for instance, during dry periods, CCI-SM shows clear wetter conditions than observed; as well as during the 2013 winter, CCI-SM is not able to capture the sudden increment of soil moisture. The sudden rise of soil moisture could be the result of frozen soil condition, which affects the accuracy of satellite data [57]. It should be noted since the study area only has one soil moisture station that provides valid observations, it is impossible to quantitatively evaluate the CCI-SM in this study. However, the temporal comparison does indicate a general agreement between the CCI-SM and the ground observations.

V. LANDSLIDE EVENTS AND RELATIONSHIPS WITH CCI-SM

To investigate the influence of soil moisture condition on landslides, we use the wetness conditions measured on the day when landslides occurred. The reason for not using the antecedent soil moisture condition plus rainfall data on the day is because the purpose of this study is to explore the relationship between soil moisture and landslides solely. In general, soil moisture is a predisposing factor for slope instability, while rainfall is the triggering factor. The same rainfall can trigger or not a landslide depending on the soil moisture content at the time of the rainfall event. The wetness conditions measured on the day of the landslide implicitly account for both the initial soil moisture and the effective rainfall absorbed by the ground, and can be a robust indicator of the hydrological condition of the slope. Only after the evaluation of the soil moisture product, rainfall information can then be used together with the antecedent soil moisture information for forecasting and monitoring purposes. After investigating the soil moisture conditions over all the satellite grids, it has been found during most of the landslide events, the soil is always among those wettest days within a year. Here the results of the four selected satellite grids are presented (Figure 5). From the figure, it can be seen soil moisture in correspondence to landslide events (in red star points) is most often in the top third range of the areal soil moisture (blue lines). It is clear the soil moisture variations at each satellite grids behave differently, for instance Figure 5a is generally wetter than Figure 5d. Therefore, it is necessary to investigate the relationship between landslides and soil moisture based on different grids. A comparison between landslide soil wetness conditions and the satellite grids soil moisture at 95%, 90%, 80%, 70%, 60%, and 50% percentiles are hence explored (Figure 6). It is interesting to observe that several landslide events occurred at very low soil moisture conditions. This is because soil moisture is not the only factor responsible for landslide. The stability of a slope, in fact, is influenced by a number of different factors such as deforestation, river erosion, or human activities that in some cases can prevail slope hydrology. The percentage of landslide events that exceed the conditioned (i.e., different percentiles) grid soil moisture is also calculated as shown in Table I. It is clear over half of the events are above the 80% percentile line, and over four-fifths of events are above the 50% percentile line. Those results indicate high soil moisture indeed plays an important role in triggering landslides.

VI. THE EVALUATION OF SOIL MOISTURE THRESHOLDS FOR LANDSLIDE OCCURRENCES

A. Whole Study Area

The above analysis has shown that there is a correlation between landslide events and soil moisture product CCI-SM. The next step is to establish if the spatial variation of soil moisture can be used to improve the thresholds for landslides occurrence at the regional scale.

As a first attempt, we can compute the critical soil moisture for landslide occurrences over the whole study region. With a 5% exceedance probability, which is commonly adopted for landslide threshold studies to exclude the outlier cases [36]. The threshold for the whole region is 0.23 m^3/m^3, which is smaller than the areal mean soil moisture at 0.33 m^3/m^3. This is because in mountainous regions, landslides can be triggered at relatively low soil moisture due to the influence of other instability factors.

Using one single threshold for the whole area is clearly not appropriate. For instance, some areas are always wetter than others, and that does not indicate those areas are more prone to landslides (e.g., wetter soil due to irrigation does not link with a high occurrence of landslides). Therefore, in order to identify landslides susceptibility, it is important to investigate how the different environmental factors can influence the soil moisture threshold. Here land cover, soil type, and slope information are taken into considerations.

TABLE II
RAINFALL EVENTS INFORMATION

Starting date			Ending date			Duration (days)	Rainfall intensity (mm/day)	Number of Landslide events
Year	Month	Day	Year	Month	Day			
2014	1	13	2014	1	24	12	20.50	2
2014	1	28	2014	2	14	18	13.61	0
2014	2	26	2014	3	6	9	13.35	0
2014	3	22	2014	3	27	6	11.08	0
2014	4	4	2014	4	5	2	18.98	0
2014	4	27	2014	5	4	8	12.13	0
2014	5	26	2014	6	3	9	5.05	0
2014	6	14	2014	6	16	3	18.29	0
2014	6	25	2014	6	30	6	11.39	0
2014	7	7	2014	7	14	8	7.84	0
2014	7	21	2014	7	30	10	15.35	0
2014	8	31	2014	9	5	6	5.67	0
2014	9	10	2014	9	12	3	11.84	0
2014	9	19	2014	9	20	2	23.04	0
2014	10	1	2014	10	1	1	14.51	0
2014	10	10	2014	10	17	8	13.01	0
2014	11	4	2014	11	18	15	18.28	0
2014	11	25	2014	12	7	13	7.58	0
2014	12	13	2014	12	16	4	6.24	0
2015	1	16	2015	1	17	2	14.87	0
2015	1	21	2015	1	23	3	7.13	0
2015	1	29	2015	2	10	13	9.98	0
2015	2	13	2015	2	17	5	6.62	1
2015	2	21	2015	2	26	6	11.84	4
2015	3	3	2015	3	7	5	11.69	1
2015	3	15	2015	3	17	3	9.00	0
2015	3	21	2015	3	27	7	12.09	2
2015	4	3	2015	4	5	3	16.62	0
2015	4	17	2015	4	18	2	6.99	0
2015	4	26	2015	4	29	4	11.23	0
2015	5	15	2015	5	16	2	8.83	0
2015	5	20	2015	5	27	8	10.58	1
2015	6	8	2015	6	11	4	6.47	0
2015	6	16	2015	6	19	4	13.44	0
2015	6	23	2015	6	24	2	6.07	0
2015	7	22	2015	7	25	4	6.05	0
2015	8	9	2015	8	10	2	24.69	0
2015	8	15	2015	8	19	5	10.69	0
2015	8	23	2015	8	24	2	7.88	0
2015	9	13	2015	9	14	2	24.66	1
2015	9	23	2015	9	24	2	7.50	0
2015	10	1	2015	10	7	7	13.73	0
2015	10	10	2015	10	19	10	9.40	0
2015	10	27	2015	10	29	3	20.33	0
2015	11	21	2015	11	25	5	13.78	1

B. Land Cover Discriminations

Land cover can play an important role in the occurrence of landslides. To study the effects of land cover on landslide, the study area is first categorised into 20 land cover types based on the selected land cover map (Figure 7). It is found the Herbaceous areas have the largest extent (37%), followed by Tree (22%), Cropland (21%), and other types. However, from Figure 8a, it can be seen the largest number of landslides occur under the Tree cover (n = 88) and the Cropland (n = 40), and Herbaceous is only on the fourth place (n = 32). Moreover, although Mosaic cropland makes up only 6% of the overall land use, the number of landslides occurred on it is relatively high (n = 37). The reason is that Mosaic cropland is mostly found in the high mountainous area, whereas the Herbaceous is mainly in the plain area. Some landslides also occurred in urban areas (six events during the study period). The soil moisture triggering levels for each land cover type are explored. The CCI-SM product can be used to evaluate the soil moisture threshold associate to each land cover type. For this purpose, land cover data has been rescaled to the CCI grid, that is, land cover types with small coverages are aggregated to those with large coverages. As a result, there is a total of three major land cover types remained: Cropland, Herbaceous and Tree cover. The corresponding soil moisture threshold at 5% exceedance are 0.23 m^3/m^3, 0.24 m^3/m^3, and 0.22 m^3/m^3. It is clear there are no distinct differences in the soil moisture thresholds among the various land covers. One possible reason is the peculiar spatial distribution of the three land cover types. Although Cropland and Herbaceous are mainly in the plain areas, and Tree cover is mainly in the mountainous regions, they all have some parts distributed outside of their major zones (i.e., Cropland and Herbaceous have some areas covered in mountainous zones, while Tree cover is also found in the plain areas). As a result, their thresholds are similar to the one over the whole area. Hence the use of the land cover feature for discriminating soil moisture thresholds is not suitable in this case.

C. Soil Type Discriminations

Different types of soil have different physical-mechanical properties that affect the hydrologic response to rainfall and the stability of the slope (e.g., soil permeability, cohesion force, shear strength and etc.). To study the effects of soil types on landslides, the study area is divided into 21 soil regions based on the soil map shown in Figure 9. From the map, it can be seen the Gleyic Solonetz covers the largest area (70%), followed by the Fibric Histosols (13%), the Haplic Andosols (7%), the Haplic Phaeozems (6%), and other types. Similarly, the number of landslide events under Gleyic Solonetz type is also the highest (Figure 8b). However, the second most frequent class is by Haplic Phaeozems. Compare with the coverage area of Haplic Phaeozems in the study region, the number of induced landslides is extremely high. This is because Haplic Phaeozems is mainly found on steep, unstable slopes made of loose material derived from the weathering weak sandstone-pelite rocks. Due to the small extent of Haplic Phaeozems in the region (aggregated by data rescaling procedure), only the Gleyic Solonetz type remains for the evaluation of the soil mositure threshold. The threshold for Gleyic Solonetz is calculated to be 0.23 m^3/m^3, which is the same as one found through the whole area exploration. This result is expected, as Gleyic Solonetz holds the most landslide events and covers the majority areas. However only one threshold is clearly not useful, as hazards can also occur in the Haplic Phaeozems type. Therefore, soil type is not recommended for the discrimination of soil moisture thresholds in this study area.

D. Slope Angle Discriminations

Slope angle is one of the most important factors that controls the stability of a slope. Therefore, it is useful to investigate the relationship between slope angle and landslides occurrence in the study area. The slope angle map of the Emilia-Romagna region is generated using the selected DEM data as illustrated in Figure 10. It can be seen the slope angle can exceeds 50° in

TABLE III
THE RESULTS OF TP, FN, FP, TN, AND STATISTICAL INDICATORS (HR, FAR, HK, D), UNDER DIFFERENT EXCEEDANCE PROBABILITY LEVELS (P). THE BEST PERFORMANCES OF HK AND D ARE HIGHLIGHTED

P (%).	TP	FN	FP	TN	HR	FAR	HK	d
1	13	0	5349	313	1.00	0.94	0.055	0.94
2	13	0	5227	435	1.00	0.92	0.077	0.92
3	13	0	5057	605	1.00	0.89	0.107	0.89
4	13	0	5004	658	1.00	0.88	0.116	0.88
5	13	0	4936	726	1.00	0.87	0.128	0.87
6	13	0	4742	920	1.00	0.84	0.162	0.84
7	13	0	4623	1039	1.00	0.82	0.184	0.82
8	13	0	4471	1191	1.00	0.79	0.210	0.79
9	13	0	4384	1278	1.00	0.77	0.226	0.77
10	13	0	4341	1321	1.00	0.77	0.233	0.77
15	13	0	3947	1715	1.00	0.70	0.303	0.70
20	13	0	3535	2127	1.00	0.62	0.376	0.62
25	12	1	3325	2337	0.92	0.59	0.336	0.59
30	12	1	2858	2804	0.92	0.50	**0.418**	**0.51**
35	10	3	2731	2931	0.77	0.48	0.287	0.53
40	9	4	2629	3033	0.69	0.46	0.228	0.56
50	7	6	2208	3454	0.54	0.39	0.148	0.60

some areas. Steep zones are mainly found near the river valley areas and at close to the main watershed divide at the Southern boundary. To work with the CCI-SM, slope data has been rescaled (i.e., averaged) to the CCI grids accordingly. Furthermore, for the purpose of thresholds calculations, slope data has been statistically divided into four groups, so all groups hold the same amount of coverage areas. It can be seen in Figure 8c, the landslides numbers agree with the average slope angle: the steeper the area, the higher the number of the landslide incidences. The soil moisture thresholds are then calculated for the different slope groups. Since group 0.40-0.84 ° only has one landslide event reported, it is removed from the analysis. As a result, the thresholds for the remained three groups are: 0.84-4.15° (0.37 m^3/m^3), 4.15- 11.23° (0.24 m^3/m^3), and 11.23-20.44° (0.20 m^3/m^3). It can be seen that the threshold differences between the plain areas and the steep areas are significant (i.e., 85% higher). The distinct results indicate the usefulness of slope information for thresholds discriminations. The spatial distribution of the calculated thresholds can be then generated (Figure 11). The map clearly shows that the critical soil moisture content is lower for the steep slopes that characterize the southern part of the region (close to watershed divide) around the hilly Southern boundary, and higher for the mild slopes to the North. This result well agrees with the general geology of the area, that in the southern part is characterised by the outcrop of sandstone rocks that form steep slopes covered by a thin layer of permeable sandy soil. These slopes are highly unstable, and commonly fail at low water content because of the steepness and the high hydraulic conductivity of the soil. The thresholds calculated via the slope angle discrimination method is then validated in the next section.

It is noted although it should be more informative to use the original slope data (from the 90 m DEM data) for each of the landslide event than the mean-slope method, we have found such an approach could not provide distinct thresholds among slope groups. This is because their corresponding soil moisture grid is large (0.25-degree), so for instance, if five landslides distributed in both high- and low-slope areas occurred within a CCI-SM grid, they would be assigned with the same soil moisture value. Therefore, in this case only the mean-slope method is further proceeded.

E. The Validation of Thresholds Using Slope Angle Discrimination Conditions

A preliminary threshold model for landslides occurrence at regional scale can be derived by combining the average slope angle and the CCI soil moisture. The threshold is here defined as the critical value of soil moisture above which landslides are likely to occur. These values are different for the different territorial units according to the average value of slope angle.

In this assessment, it is important to optimize the threshold values of soil moisture in order to reduce the number of missing alarms (when the threshold is too high) and false alarms (when the threshold is too low). In our case, we use the slope angle as discrimination conditions and consider 17 different exceedance probabilities (from 1% to 50%). The validation is then carried out to test the thresholds under 45 rainfall events (Table II). The rainfall events are in the ranges of 1 day to 18 days, and the average rainfall intensities are between 5.05 mm/day and 24.69 mm/day. During each event, the number of landslides occurred is also shown. In combination with the satellite grids, there is a total of 5662 different outcomes of the TP, FN, FP and the TN. The statistical scores are calculated based on those outcomes, and ROC analysis is also carried out. Table III summaries the results of TP, FN, FP and TN, as well as the four statistical indicators of HR, FAR, HK, and d for the 17 cases. Taking a 5% exceedance probability, all the occurred landslides (13 recorded landslide events) during the selected rainfall events are predicted by the thresholds (TP); however the FP is very high (4936 cases). Accordingly, for the 5% exceedance probability, HR=1.00 and FAR=0.87. With an exceedance probability of 50%, the HR drops from 1.00 (13 TP and zero FN) to 0.54 (seven TP and six FN), while the FAR improves from 0.94 (5349 FP and 313 TN) to 0.39 (2208 FP and 3454 TN). The worst HK result is observed in 1% scenario (HK=0.055), while the best one is obtained by the 30% scenario (HK=0.418). The ROC curve is plotted in Figure 12. In the figure, each blue point represents a scenario with a selected exceedance probability level. The top flat part of the curve corresponds to HR=1.00 scenarios (1-20% exceedance probability levels). It can be seen with different exceedance probabilities, FAR can be reduced without sacrificing the HR rate. The Euclidean distances d between blue points and the optimal point (the red dot) are also calculated as shown in Table III. Similar to the HK performance, the largest distance is again observed by the 1% scenario (d = 0.94), while the smallest distance is achieved by the 30% scenario (d = 0.51). Based on the HK result, the most suitable thresholds are obtained by the 30% exceedance probability.

VII. Discussions and Conclusions

In this study, the relationship between the CCI-SM and the landslide events has been assessed in the Emilia Romagna region for the period between 2002 and 2015. Additionally, attempts have been made to find the soil moisture thresholds for landslides occurrences under different environmental conditions (i.e., land cover, soil type, and slope). Specifically, the temporal comparison between CCI-SM and in-situ observations shows a general agreement between the datasets. A clear relationship has been found between the CCI-SM and the landslide events, as over half of the landslide events occur above the wettest 20% soil moisture, and over four-fifths of events occur above the wettest 50% soil moisture. Those results indicate high CCI-SMs indeed relate to the triggering of landslides. Detailed analysis of the environmental features allows identifying a few differences between thresholds. Of the three factors used, only the slope distribution results in a clear separation of the thresholds, with thresholds becoming smaller for steeper areas. The empirical evidence confirms that wetter soil is required to trigger landslides in milder slopes than in steeper slopes. The fact that the slope is more distinctive than the other environmental conditions (land cover and soil type) should not be surprising, as the slope is a key factor for earth stabilities. Further validation studies based on the slope discrimination conditions is then carried out, which is important to reduce the false predictions. 17 different exceedance probability levels from 1% to 50% are used to explore the best thresholds scenario. Selection of the optimal threshold is based on three statistical indicators, and the results demonstrate the best performance is obtained by the 30% exceedance probability.

It is important to point out the validation conclusion made here is based on the best compromise between the minimum number of incorrect landslide predictions (FP and FN) and the maximum number of correct predictions (TP and TN) without considering additional weighting factors. However, in real applications, weightings should be considered, for example the cost of missing alarms could be much more expensive than the cost of false alarms or vice versa. Therefore, thresholds decision makings at different regions should depend on the cost of each situation accordingly. On the other hand, the impacts of hazards at one region can also be distinct at different times, for example a school over the weekends or holidays, when no one need to be evacuated should have totally different sets of thresholds when comparing with the one during the term-times. Therefore, thresholds should change both spatially and temporally (i.e., dynamically). To realise such a target, an agent-based dynamic model could be very useful, and the results found in this study can be put into such a model for landslide hazards early warnings [58].

Although our study shows a clear relationship between the CCI-SM and the landslide occurrences, the temporal coverage of CCI-SM for the study region is still limited. CCI is aimed at producing long-term over 30 years soil moisture data globally, however, in the study area, the data are mostly unavailable before the year 2002. Comparing with the comprehensive data records of the landslide which started in the year 1899, the shorter coverage of satellite data leads to a large cut of usable landslides cases. This is because satellites dedicated for soil moisture observations are only initiated in 2002, with the launch of AMSR-E. The data scarcity issue could be solved by fusing satellite data with land surface modelled soil moisture (e.g., Noah-Multiparameterization Land

Surface Model) to provide an extended period of datasets. Machine learning technologies [59] such as Support Vector Machines could be used for such purposes.

Since satellite soil moisture observations are only representative of a shallow soil layer, it limits their usage in hydrological and landslide applications. One potential approach to minimise the problem is by using the exponential filter (also called Soil Water Index) to calculate the corresponding root-zone soil moisture [60]. An exploration has been carried out by using the recursive formulation as described in [60]. It has been found the resultant root-zone soil moisture (the optimal T parameter is determined as 2 days) cannot perform as well as the original CCI-SM data for landslide predictions. The main reason we suspect is due to the large data gaps in the CCI-SM product (i.e., CCI-SM is not continuously available, and sometimes the data gap can be more than 10 days), therefore the exponential filter equation which largely depends on the soil moisture data from the last time step is not suitable in this case. However, if in the future satellites are capable of providing more temporally consistent soil moisture observations, the suggested method could have the potential to provide good landslide prediction results.

Furthermore, it has been found the large grid sizes of satellite data can hinder the further environmental threshold studies, because feature types with small coverage areas are aggregated by those with large coverages areas (i.e., a large number of landslide events have been reported in the Haplic Phaeozems soil type, but due to its small coverage area, threshold cannot be calculated). A potential solution is to increase the satellite data resolution by downscaling methodologies. Higher resolution data sources such as satellite visible/ infrared data can be used for such a purpose.

Another issue is related to the landslide data. Since most landslide catalogs only record events that are experienced by people (e.g., from victims, local newspapers, and reports), many events in the rural areas are undetected. As a result, when investigating the soil moisture thresholds, the outcome could be biased, i.e., the false alarm can be inaccurately high. In order to expand the catalog, remote sensing images and Geographical Information Systems (GIS) can be useful.

With the encouraging results obtained, future investigations will be to use the satellite antecedent soil moisture information, together with rainfall data (e.g., rainfall thresholds or forecasted rainfall data) for landslide early warning. Moreover, satellite soil moisture data can also be used in physically based models for landslides predictions. The results presented here are only valid for this specific investigated case study, therefore further studies analysing the relationship between satellite soil moisture and landslides over a wider range of catchments and with more environmental features are needed.

REFERENCES

[1] M. Klose, L. Highland, B. Damm, and B. Terhorst, "Estimation of Direct Landslide Costs in Industrialized Countries: Challenges, Concepts, and Case Study," in World Landslide Forum 3, China (Beijing), 2014, pp. 661-667: Springer International Publishing.

[2] M. Scaioni, L. Longoni, V. Melillo, and M. Papini, "Remote Sensing for Landslide Investigations: An Overview of Recent Achievements and Perspectives," Remote Sensing, vol. 6, no. 10, p. 9600, 2014.

[3] R. L. Schuster, "Landslides: Investigation and Mitigation," vol. 247, A. K. Turner and R. L. Schuster, Eds. Transportation Research Board Special: National Academy Press: Washington, DC, USA, 1996, pp. 12-35.

[4] P. Canuti, N. Casagli, L. Ermini, R. Fanti, and P. Farina, "Landslide activity as a geoindicator in Italy: significance and new perspectives from remote sensing," Environmental Geology, vol. 45, no. 7, pp. 907-919, 2004.

[5] N. Caine, "The rainfall intensity-duration control of shallow landslides and debris flows," Geografiska annaler: series A, physical geography, vol. 62, no. 1-2, pp. 23-27, 1980.

[6] T. Glade, M. Crozier, and P. Smith, "Applying probability determination to refine landslide-triggering rainfall thresholds using an empirical “Antecedent Daily Rainfall Model”," Pure and Applied Geophysics, vol. 157, no. 6-8, pp. 1059-1079, 2000.

[7] M. J. Crozier, "Prediction of rainfall - triggered landslides: A test of the antecedent water status model," Earth surface processes and landforms, vol. 24, no. 9, pp. 825-833, 1999.

[8] T.-L. Tsai and H.-F. Chen, "Effects of degree of saturation on shallow landslides triggered by rainfall," Environmental Earth Sciences, vol. 59, no. 6, pp. 1285-1295, 2010.

[9] R. Hawke and J. McConchie, "In situ measurement of soil moisture and pore-water pressures in an ‘incipient’landslide: Lake Tutira, New Zealand," Journal of environmental management, vol. 92, no. 2, pp. 266-274, 2011.

[10] M. Bittelli, R. Valentino, F. Salvatorelli, and P. R. Pisa, "Monitoring soil-water and displacement conditions leading to landslide occurrence in partially saturated clays," Geomorphology, vol. 173, pp. 161-173, 2012.

[11] S. Segoni, A. Rosi, D. Lagomarsino, R. Fanti, and N. Casagli, "Brief communication: Using averaged soil moisture estimates to improve the performances of a regional-scale landslide early warning system," Natural Hazards and Earth System Sciences, vol. 18, no. 3, pp. 807-812, 2018.

[12] P. Valenzuela, M. J. Domínguez-Cuesta, M. A. M. García, and M. Jiménez-Sánchez, "Rainfall thresholds for the triggering of landslides considering previous soil moisture conditions (Asturias, NW Spain)," Landslides, vol. 15, no. 2, pp. 273-282, 2018.

[13] T. Bogaard and R. Greco, "Invited perspectives: Hydrological perspectives on precipitation intensity-duration thresholds for landslide initiation: proposing hydro-meteorological thresholds," Natural Hazards and Earth System Sciences, vol. 18, no. 1, pp. 31-39, 2018.

[14] A. F. Chleborad, "Preliminary evaluation of a precipitation threshold for anticipating the occurrence of landslides in the Seattle, Washington, Area," US Geological Survey open-file report, vol. 3, no. 463, p. 39, 2003.

[15] M. Calvello, R. N. d’Orsi, L. Piciullo, N. Paes, M. Magalhaes, and W. A. Lacerda, "The Rio de Janeiro early warning system for rainfall-induced landslides: analysis of performance for the years 2010–2013," International journal of disaster risk reduction, vol. 12, pp. 3-15, 2015.

[16] J. L. Zêzere, R. M. Trigo, and I. F. Trigo, "Shallow and deep landslides induced by rainfall in the Lisbon region (Portugal): assessment of relationships with the North Atlantic Oscillation," Natural Hazards and Earth System Science, vol. 5, no. 3, pp. 331-344, 2005.

[17] J. D. Pelletier, B. D. Malamud, T. Blodgett, and D. L. Turcotte, "Scale-invariance of soil moisture variability and its implications for the frequency-size distribution of landslides," Engineering Geology, vol. 48, no. 3-4, pp. 255-268, 1997.

[18] R. L. Baum and J. W. Godt, "Early warning of rainfall-induced shallow landslides and debris flows in the USA," Landslides, vol. 7, no. 3, pp. 259-272, 2010.

[19] L. Brocca, F. Melone, and T. Moramarco, "On the estimation of antecedent wetness conditions in rainfall–runoff modelling," Hydrological Processes: An International Journal, vol. 22, no. 5, pp. 629-642, 2008.

[20] L. Zhuo and D. Han, "Misrepresentation and amendment of soil moisture in conceptual hydrological modelling," Journal of Hydrology, vol. 535, pp. 637-651, 2016.

[21] L. Zhuo and D. Han, "Could operational hydrological models be made compatible with satellite soil moisture observations?," Hydrological Processes, vol. 30, no. 10, pp. 1637-1648, 2016.

[22] R. Greco, A. Guida, E. Damiano, and L. Olivares, "Soil water content and suction monitoring in model slopes for shallow flowslides early warning applications," Physics and Chemistry of the Earth, Parts A/B/C, vol. 35, no. 3-5, pp. 127-136, 2010.

[23] S. Harris, R. Orense, and K. Itoh, "Back analyses of rainfall-induced slope failure in Northland Allochthon formation," Landslides, vol. 9, no. 3, pp. 349-356, 2012.

[24] A. J. Posner and K. P. Georgakakos, "Soil moisture and precipitation thresholds for real-time landslide prediction in El Salvador," Landslides, vol. 12, no. 6, pp. 1179-1196, 2015.
[25] L. Brocca, L. Ciabatta, T. Moramarco, F. Ponziani, N. Berni, and W. Wagner, "Use of satellite soil moisture products for the operational mitigation of landslides risk in central Italy," in Satellite Soil Moisture Retrieval: Elsevier, 2016, pp. 231-247.
[26] L. Zhuo, D. Han, Q. Dai, T. Islam, and P. K. Srivastava, "Appraisal of NLDAS-2 multi-model simulated soil moistures for hydrological modelling," Water resources management, vol. 29, no. 10, pp. 3503-3517, 2015.
[27] L. Zhuo and D. Han, "Hydrological evaluation of satellite soil moisture data in two basins of different climate and vegetation density conditions," Advances in Meteorology, vol. 2017, 2017.
[28] L. Zhuo, Q. Dai, T. Islam, and D. Han, "Error distribution modelling of satellite soil moisture measurements for hydrological applications," Hydrological Processes, vol. 30, no. 13, pp. 2223-2236, 2016.
[29] L. Zhuo, D. Han, and Q. Dai, "Soil moisture deficit estimation using satellite multi-angle brightness temperature," Journal of Hydrology, vol. 539, pp. 392-405, 2016.
[30] L. Zhuo, D. Han, and Q. Dai, "Exploration of empirical relationship between surface soil temperature and surface soil moisture over two catchments of contrasting climates and land covers," Arabian Journal of Geosciences, vol. 10, no. 18, p. 410, 2017.
[31] L. Brocca, F. Ponziani, T. Moramarco, F. Melone, N. Berni, and W. Wagner, "Improving landslide forecasting using ASCAT-derived soil moisture data: A case study of the Torgiovannetto landslide in central Italy," Remote Sensing, vol. 4, no. 5, pp. 1232-1244, 2012.
[32] R. L. Ray and J. M. Jacobs, "Relationships among remotely sensed soil moisture, precipitation and landslide events," Natural Hazards, vol. 43, no. 2, pp. 211-222, 2007.
[33] R. L. Ray, J. M. Jacobs, and M. H. Cosh, "Landslide susceptibility mapping using downscaled AMSR-E soil moisture: A case study from Cleveland Corral, California, US," Remote sensing of environment, vol. 114, no. 11, pp. 2624-2636, 2010.
[34] R. L. Ray, J. M. Jacobs, and T. P. Ballestero, "Regional landslide susceptibility: spatiotemporal variations under dynamic soil moisture conditions," Natural hazards, vol. 59, no. 3, pp. 1317-1337, 2011.
[35] F. Ponziani, C. Pandolfo, M. Stelluti, N. Berni, L. Brocca, and T. Moramarco, "Assessment of rainfall thresholds and soil moisture modeling for operational hydrogeological risk prevention in the Umbria region (central Italy)," Landslides, vol. 9, no. 2, pp. 229-237, 2012.
[36] S. Peruccacci, M. T. Brunetti, S. L. Gariano, M. Melillo, M. Rossi, and F. Guzzetti, "Rainfall thresholds for possible landslide occurrence in Italy," Geomorphology, vol. 290, pp. 39-57, 2017.
[37] W. Dorigo et al., "ESA CCI Soil Moisture for improved Earth system understanding: State-of-the art and future directions," Remote Sensing of Environment, vol. 203, pp. 185-215, 2017.
[38] C. Pratola, B. Barrett, A. Gruber, G. Kiely, and E. Dwyer, "Evaluation of a global soil moisture product from finer spatial resolution SAR data and ground measurements at Irish sites," Remote Sensing, vol. 6, no. 9, pp. 8190-8219, 2014.
[39] C. Albergel et al., "Skill and global trend analysis of soil moisture from reanalyses and microwave remote sensing," Journal of Hydrometeorology, vol. 14, no. 4, pp. 1259-1277, 2013.
[40] R. An et al., "Validation of the ESA CCI soil moisture product in China," International journal of applied earth observation and geoinformation, vol. 48, pp. 28-36, 2016.
[41] M. Berti, M. Martina, S. Franceschini, S. Pignone, A. Simoni, and M. Pizziolo, "Probabilistic rainfall thresholds for landslide occurrence using a Bayesian approach," Journal of Geophysical Research: Earth Surface, vol. 117, no. F4, 2012.
[42] D. Lagomarsino, S. Segoni, R. Fanti, and F. Catani, "Updating and tuning a regional-scale landslide early warning system," Landslides, vol. 10, no. 1, pp. 91-97, 2013.
[43] esa. (2018, 07 Jul). Release of ESA CCI SM v04.2 – a new era of global soil moisture.
[44] A. Pistocchi, F. Bouraoui, and M. Bittelli, "A simplified parameterization of the monthly topsoil water budget," Water Resources Research, vol. 44, no. 12, 2008.
[45] F. Karsli, M. Atasoy, A. Yalcin, S. Reis, O. Demir, and C. Gokceoglu, "Effects of land-use changes on landslides in a landslide-prone area (Ardesen, Rize, NE Turkey)," Environmental monitoring and assessment, vol. 156, no. 1-4, p. 241, 2009.
[46] A. Di Gregorio, Land cover classification system: classification concepts and user manual: LCCS. Food & Agriculture Org., 2005.
[47] T. Hengl et al., "SoilGrids250m: Global gridded soil information based on machine learning," PLoS one, vol. 12, no. 2, p. e0169748, 2017.
[48] P. Berry, J. Garlick, and R. Smith, "Near-global validation of the SRTM DEM using satellite radar altimetry," Remote Sensing of Environment, vol. 106, no. 1, pp. 17-27, 2007.
[49] Q. Dai, D. Han, M. Rico-Ramirez, and P. K. Srivastava, "Multivariate distributed ensemble generator: A new scheme for ensemble radar precipitation estimation over temperate maritime climate," Journal of Hydrology, vol. 511, pp. 17-27, 2014.
[50] Q. Dai, D. Han, M. A. Rico‐Ramirez, L. Zhuo, N. Nanding, and T. Islam, "Radar rainfall uncertainty modelling influenced by wind," Hydrological processes, vol. 29, no. 7, pp. 1704-1716, 2015.
[51] Q. Dai, D. Han, L. Zhuo, J. Zhang, T. Islam, and P. K. Srivastava, "Seasonal ensemble generator for radar rainfall using copula and autoregressive model," Stochastic environmental research and risk assessment, vol. 30, no. 1, pp. 27-38, 2016.
[52] S. L. Gariano et al., "Calibration and validation of rainfall thresholds for shallow landslide forecasting in Sicily, southern Italy," Geomorphology, vol. 228, pp. 653-665, 2015.
[53] D. Wilks, Statistical Methods in the Atmospheric Sciences, 3rd ed. Academic Press, 2011.
[54] A. Hanssen and W. Kuipers, On the Relationship Between the Frequency of Rain and Various Meteorological Parameters:(with Reference to the Problem Ob Objective Forecasting). Staatsdrukkerij-en Uitgeverijbedrijf, 1965.
[55] D. Hosmer and S. Lemeshow, "Applied logistic regression. 1989," New York: Johns Wiley & Sons, 1989.
[56] T. Fawcett, "An introduction to ROC analysis," Pattern recognition letters, vol. 27, no. 8, pp. 861-874, 2006.
[57] L. Zhuo, Q. Dai, and D. Han, "Evaluation of SMOS soil moisture retrievals over the central United States for hydro-meteorological application," Physics and Chemistry of the Earth, Parts A/B/C, vol. 83, pp. 146-155, 2015.
[58] R. J. Dawson, R. Peppe, and M. Wang, "An agent-based model for risk-based flood incident management," Natural hazards, vol. 59, no. 1, pp. 167-189, 2011.
[59] L. Zhuo and D. Han, "Multi-source hydrological soil moisture state estimation using data fusion optimisation," Hydrology and Earth System Sciences, vol. 21, no. 7, pp. 3267-3285, 2017.
[60] C. Albergel et al., "From near-surface to root-zone soil moisture using an exponential filter: an assessment of the method based on in-situ observations and model simulations," Hydrology and Earth System Sciences, vol. 12, no. 6, pp. 1323-1337, 2008.

Lu Zhuo (M'88) received her MEng Civil Engineering degree (2011) and PhD degree in Civil Engineering (2016) at the University of Bristol, UK (UoB). She is currently working as a Research Associate on the Resilient Economy and Society by Integrated SysTems modelling (RESIST) project at the UoB (2016-current). Her research areas include multiple natural hazards modelling and monitoring (e.g., floods, landslides, and earthquake), remote sensing of environment, and disaster risk management. She has published over 30 peer-reviewed journal and conference papers including in high impact journals such as Journal of Hydrology, Hydrological Processes and Hydrology and Earth System Sciences.

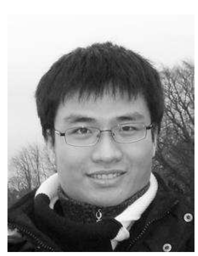

Qiang Dai (M'87) received the B.S. degree in Geography from Nanjing Normal University, China, in 2009, the M.S. degree in Geography and Planning from Sun Yat-sen University, China, in 2011, and the PhD degree in Civil Engineering from University of Bristol, UK, in 2014. From 2014 to 2017, he was an Associate Professor with the Nanjing Normal University. Since 2017, he has been a Research Associate with the Civil Engineering Department, University of Bristol, UK. His research interest includes the rainfall estimate and forecast based on weather radar and numerical weather prediction, urban flood forecasting, and multi-hazards modelling. Key expertise within the centre exists in meteorology, hazards, radar hydrology and numerical weather prediction model.

Dawei Han was born in Tianjin City, China, in 1961. He received his BEng (1982) and MSc (1984) degrees in Water Conservancy from North China University of Water Conservancy and Electric Power, and PhD (1991) in radar hydrology from the University of Salford, UK. He is currently Professor of Hydroinformatics in the department of Civil Engineering, University of Bristol, UK. His research areas include Hydroinformatics, Real-time Flood Forecasting, Flood Risk Management, Remote Sensing and Geographic Information System, natural hazards, and water resources management. He has carried out various projects on weather radar rainfall and numerical weather prediction to aid flood risk assessment, downscaling of global circulation model for climate change, multi-natural hazards, etc. He has published over 200 peer-reviewed journal and conference papers. For further details: http://www.bristol.ac.uk/engineering/people/dawei-han/index.html.

Ningsheng Chen (M' 65) obtained PhD at the Institute of Mountain Hazards and Environment (IMHE), China in early 1990s. He is currently Professor of Physical Geography in IMHE. His research interests are: the mechanism of mountain disaster formation and engineering prevention and control technology, monitoring and early warning and forecasting technology. He has published >90 journal papers, including 31 high-impact papers published in Remote Sensing and Environment, Geomorphology, The Holocene, and Landslide etc. For further details, please see http://sourcedb.imde.cas.cn/yw/rc/fas/200908/t20090806_2332963.html.

Binru Zhao was born in Shanxi, China in 1992. She received the B.S. degree in civil engineering from Hohai University, Nanjing, China, in 2014 and then started pursuing the Ph.D. degree in civil engineering at Hohai University, Nanjing, China. She is currently a visiting student at the University of Bristol, Bristol, UK.

Matteo Berti (M'87) received the M.S. degree in Geology from the University of Bologna, Italy, in 1992, and the Ph.D. degree in Engineering Geology from the University of Ferrara, Italy, in 1997. From 2004 to 2014, he was Research Assistant at the Earth Science Department of the University of Bologna, then Associate Professor from 2015 to 2016. Since 2017, he is Full Professor of Engineering Geology at the same department. He is author of more 70 articles in peer-reviewed journals. His research interests include: the hydrological response of slopes to rainfall; the deterministic, probabilistic, and numerical modelling of slope stability problems; the triggering mechanisms and propagation of shallow landslides and debris flows; the use of satellite radar interferometry for the evaluation of the state of activity of slow-moving landslides; the analysis of the solid-to-fluid transition of earthflows; the application of slope monitoring for landslide hazard assessment.